arXiv:1411.3965v1 [astro-ph.HE] 14 Nov 2014

Mechanism of Outflows in Accretion System: Advective Cooling Cannot Balance Viscous Heating?

Wei-Min Gu

Department of Astronomy and Institute of Theoretical Physics and Astrophysics, Xiamen University, Xiamen, Fujian 361005, China

guwm@xmu.edu.cn

ABSTRACT

Based on no-outflow assumption, we investigate steady state, axisymmetric, optically thin accretion flows in spherical coordinates. By comparing the vertically integrated advective cooling rate with the viscous heating rate, we find that the former is generally less than 30% of the latter, which indicates that the advective cooling itself cannot balance the viscous heating. As a consequence, for radiatively inefficient flows with low accretion rates such as $\dot{M} \lesssim 10^{-3}\dot{M}_{\rm Edd}$, where $\dot{M}_{\rm Edd}$ is the Eddington accretion rate, the viscous heating rate will be larger than the sum of the advective cooling rate and the radiative cooling one. Thus, no thermal equilibrium can be established under the no-outflow assumption. We therefore argue that in such case outflows ought to occur and take away more than 70% of the thermal energy generated by viscous dissipation. Similarly, for optically thick flows with extremely large accretion rates such as $\dot{M} \gtrsim 10\dot{M}_{\rm Edd}$, outflows should also occur due to the limited advection and the low efficiency of radiative cooling. Our results may help to understand the mechanism of outflows found in observations and numerical simulations.

Subject headings: accretion, accretion disks — black hole physics — hydrodynamics — outflows

1. Introduction

Outflows may play an essential role in accretion system according to recent observations and simulations. Based on Chandra observations of Fe Kα line, Wang et al. (2013) found that outflows are significant in our own Galaxy's supermassive black hole accretion system, and only less than 1% of the original gas can be accreted by the hole. Apart from observations,

some simulations also showed that outflows exist in both optically thick and thin accretion systems. For the optically thick, super-Eddington accretion case, Ohsuga et al. (2005) performed two-dimensional radiation-hydrodynamic simulations and found that strong outflows exist and the inflow accretion rate is roughly proportional to the radius. Such a scenario was confirmed by Ohsuga & Mineshige (2011) with two-dimensional radiation-magnetohydrodynamic simulations, which also found that outflows exist in optically thin, radiatively inefficient flows. In addition, for the optically thin case, Yuan et al. (2012) showed that strong outflows exist and the inflow accretion rate can be described by $\dot{M} \propto r^s$, where s is in the range [0.4, 0.7].

Many mechanisms have been proposed to power outflows. For the optically thick system, a possible mechanism is related to the radiation pressure. With high accretion rates, the radiation force is so strong that the vertical component of gravitational force cannot balance it. Consequently, the excess radiation pressure will force a part of the accreted gas into outflows. On the other hand, for the optically thin system, the well-known advection-dominated accretion flow (ADAF, Narayan & Yi 1994) may possess a positive Bernoulli parameter owing to its high internal energy, which may account for outflows. Another mechanism is the BP process (Blandford & Payne 1982) with large-scale magnetic fields, which can work for both optically thick and thin flows.

In the present work, we will study the mechanism for powering outflows in a different way. Our main concern is why outflows have to occur in many accretion systems. During the past four decades there are three well-known and widely applied accretion models (for a review, see Kato et al. 2008), namely the standard thin disk (Shakura & Sunyaev 1973), the slim disk (Abramowicz et al. 1988, or the optically thick advection-dominated accretion flow), and the optically thin advection-dominated accretion flow (ADAF). The standard thin disk is radiative cooling dominated and it is believed that outflows are quite weak in such a model. On the contrary, the other two models are advective cooling dominated and outflows are likely to be significant. Such a phenomenon hints that there may exist some relationship between the outflows and the strength of energy advection.

As argued in Gu & Lu (2007), the classic slim disk model did not predict outflows even for extremely high accretion rates since a Taylor expansion of the vertical component of gravitational force was adopted instead of the explicit one. Such an approximate force will be greatly magnified for geometrically not thin disks and therefore be able to balance the radiation force thus suppress outflows. Once the explicit force is adopted, as shown in Figure 5 of Gu & Lu (2007), no thermal equilibrium solution can exist for high accretion rates, which implies that outflows are inevitable. The physical reason for no solution is that the advective cooling is not strong enough to balance the viscous heating. Such a work is, however, limited to optically thick flows. Moreover, some basic assumptions in this work,

such as unified radial and azimuthal velocity at a certain cylindrical radius R, may not be appropriate particularly for geometrically thick disks.

The main purpose of this work is to investigate the possibility of thermal equilibrium in accretion systems without outflows. We will focus on the optically thin flows under spherical coordinates. The paper is organized as follows. Equations and boundary conditions are derived in Section 2. Analyses of the vertical structure are presented in Section 3. Numerical results of the energy advection are shown in Section 4. The mass outflow rate is estimated in Section 5. Conclusions and discussion are made in Section 6.

2. Equations and boundary conditions

Based on the assumption that there is no outflow, we study a steady state, axisymmetric accretion flow in spherical coordinates (r, θ, ϕ) under the Newtonian potential, $\psi = -GM/r$, where M is the black hole mass. For simplicity, we assume $v_\theta = 0$, which corresponds to a hydrostatic equilibrium in the θ (or vertical) direction. Then, the momentum equations in the r, θ, and ϕ direction take the forms,

$$v_r \frac{dv_r}{dr} + \frac{1}{\rho}\frac{dp}{dr} - \frac{v_\phi^2}{r} + \frac{GM}{r^2} = 0 \ , \tag{1}$$

$$\frac{1}{\rho}\frac{dp}{d\theta} - v_\phi^2 \cot\theta = 0 \ , \tag{2}$$

$$\frac{d(rv_\phi)}{dr} - \frac{1}{r^2 \rho v_r}\frac{d(r^3 \tau_{r\phi})}{dr} = 0 \ , \tag{3}$$

where v_r and v_ϕ are respectively the radial and azimuthal velocity, ρ is the density, and p is the pressure. The $r\phi$ component of the stress tensor $\tau_{r\phi} = \nu\rho r\partial(v_\phi/r)/\partial r$, where $\nu = \alpha p r/\rho v_{\rm K}$ is the kinematic viscosity coefficient, and α is a constant viscosity parameter.

Our main focus is the vertical structure and therefore we will make some simplification in the radial direction. Following Narayan & Yi (1994), the radial self-similarity is adopted: $v_r \propto r^{-1/2}$, $v_\phi \propto r^{-1/2}$, $\rho \propto r^{-3/2}$, and $p \propto r^{-5/2}$. We would stress that, as shown by Figures 1 and 2 in Narayan et al. (1997), the self-similar solution does not perfectly match with the numerical one, especially for the region close to the inner and outer boundaries. Besides, the effects of general relativity are not considered in the present work. For the innermost part of the flow, since the gravitational force is significantly stronger in general relativity than that in the Newtonian one, the present analysis may not apply to this particular region.

In addition, in order to avoid detailed radiative process, we assume a polytropic relation $p = K\rho^\Gamma$ in the θ direction. We would point out a significant difference between the present

work and Gu et al. (2009). In Gu et al. (2009), Γ was assumed to be identical to the ratio of specific heats γ, and therefore Γ was limited to the range [4/3, 5/3]. However, some simulations (e.g., Figure 3 of Villiers et al. 2005) revealed that the density may decrease faster than the pressure from the equatorial plane to the surface, which prefers to $\Gamma < 1$. In the present work, we will study for a wider range [0.1, 1.7] for Γ and take $\Gamma = 1.5$ and $\Gamma = 0.5$ as two typical examples. With the above assumptions, the dynamic equations (1-3) are reduced to

$$\frac{1}{2}v_r^2 + \frac{5}{2}\lambda v_{\rm K}^2 \tilde{\rho}^{\Gamma-1} + v_\phi^2 - v_{\rm K}^2 = 0 \ , \tag{4}$$

$$\lambda\Gamma v_{\rm K}^2 \tilde{\rho}^{\Gamma-2}\frac{d\tilde{\rho}}{d\theta} - v_\phi^2 \cot\theta = 0 \ , \tag{5}$$

$$v_r = -\frac{3}{2}\alpha\lambda v_{\rm K}\tilde{\rho}^{\Gamma-1} \ , \tag{6}$$

where $\tilde{\rho} \equiv \rho/\rho_0$ is the dimensionless mass density, ρ_0 is the density on the equatorial plane, $\lambda \equiv (p_0/\rho_0)/v_{\rm K}^2$, and $v_{\rm K} = (GM/r)^{1/2}$ is the Keplerian velocity. The physical meaning of λ is the energy advection strength on the equatorial plane, as can be indicated by Equations (6) and (12).

By combining Equations (4-6) and eliminating v_r and v_ϕ, we can obtain the following differential equation for the density $\tilde{\rho}$,

$$\frac{d\tilde{\rho}}{d\theta} = \frac{\cot\theta}{\Gamma}\left(\frac{\tilde{\rho}^{2-\Gamma}}{\lambda} - \frac{5}{2}\tilde{\rho} - \frac{9}{8}\alpha^2\lambda\tilde{\rho}^{\Gamma}\right) \ . \tag{7}$$

Since the above first order differential equation has an unknown parameter λ, two boundary conditions are required to solve this equation. A natural condition is on the equatorial plane, i.e., $\tilde{\rho}|_{\theta=\pi/2} = 1$. The other condition can be fixed at a certain polar angle $\theta_{\rm s}$, which can be regarded as the surface of the flow. Once the density $\tilde{\rho}$ at $\theta_{\rm s}$ is given, the parameter λ as well as the vertical structure can be derived. The numerical results will be presented in Section 4.

3. Analyses

Before directly solve the equations in Section 2, we will manage to derive some analytic results. Obviously, on the right hand side of Equation (7), the third term $(-9\alpha^2\lambda\tilde{\rho}^{\Gamma}/8)$ is significantly smaller than the other two terms even for relatively high viscosity such as $\alpha = 0.1$. In our analyses, this term will be dropped and Equation (7) is therefore reduced to

$$\frac{d\tilde{\rho}}{d\theta} = \frac{\cot\theta}{\Gamma}\left(\frac{\tilde{\rho}^{2-\Gamma}}{\lambda} - \frac{5}{2}\tilde{\rho}\right) \ . \tag{8}$$

The above differential equation can be analytically integrated and the vertical profile of $\tilde{\rho}$ is expressed by

$$\frac{1-\tilde{\rho}^{\Gamma-1}}{1-\tilde{\rho}_{\rm s}^{\Gamma-1}}=\frac{\sin\theta^{-\frac{5(\Gamma-1)}{2\Gamma}}-1}{\sin\theta_{\rm s}^{-\frac{5(\Gamma-1)}{2\Gamma}}-1}\ , \tag{9}$$

where $\tilde{\rho}_{\rm s}$ is the dimensionless density at $\theta=\theta_{\rm s}$. In this work we will fix $\theta_{\rm s}=\pi/6$ and focus on the region $\pi/6\leqslant\theta\leqslant\pi/2$. Some simulations (e.g., Villiers et al. 2005; Yuan & Bu 2010) showed $\tilde{\rho}\lesssim 10^{-2}$ (or even $\lesssim 10^{-3}$) at $\theta=\pi/6$, which indicates that the region $\pi/6\leqslant\theta\leqslant 5\pi/6$ will contain most of the accreted gas. We would stress that the method here is likely to be more appropriate than that in Gu et al. (2009), since we adopt a value for $\tilde{\rho}_{\rm s}$ at $\theta_{\rm s}$ according to simulation results rather than fix $\rho=0$ and $p=0$ as boundary conditions no matter where they locate.

We will first study the vertical structure of the flows for $\Gamma=1.5$ and $\Gamma=0.5$ as two typical examples, where $\tilde{\rho}_{\rm s}=0.01$ is adopted. The vertical profiles of the density $\tilde{\rho}$, the azimuthal velocity v_ϕ, and the radial velocity v_r are plotted in Figure 1. Both Figure 1(a) and 1(b) show that the density decreases from the equatorial plane to the surface. The difference is that, for $\Gamma=1.5$, v_ϕ increases and $|v_r|$ decreases from the equatorial plane to the surface, whereas for $\Gamma=0.5$, the opposite behavior occurs. Actually, the vertical profiles with $\Gamma=1.5$ is a typical example for the case with $\Gamma>1$, and the profiles with $\Gamma=0.5$ is a typical example for the case with $\Gamma<1$. The results can be easily understood by Equations (4) and (6). The latter shows $v_r\propto\tilde{\rho}^{\Gamma-1}$, so the profile of v_r is relevant to the sign of $(\Gamma-1)$. The former shows that both the first and second terms on the left hand side are determined by $\tilde{\rho}^{\Gamma-1}$, and therefore the profile of v_ϕ is also relevant to the sign of $(\Gamma-1)$. From another point of view, if we define a sound speed as $c_{\rm s}^2=p/\rho$, then there exists $c_{\rm s}^2\propto\rho^{\Gamma-1}$. Since both v_r and v_ϕ can be expressed by $c_{\rm s}$, the opposite behavior of v_r and v_ϕ in these two panels is also related to the profile of $c_{\rm s}$, thus simply the sign of $(\Gamma-1)$.

The value of λ can also be analytically derived with given pair of $(\theta_{\rm s},\tilde{\rho}_{\rm s})$,

$$\lambda=\frac{2}{5}\frac{\sin\theta_{\rm s}^{-\frac{5(\Gamma-1)}{2\Gamma}}-1}{\sin\theta_{\rm s}^{-\frac{5(\Gamma-1)}{2\Gamma}}-\tilde{\rho}_{\rm s}^{\Gamma-1}}\ . \tag{10}$$

The variation of λ with Γ for $\tilde{\rho}_{\rm s}=0.1$, 0.01, and 0.001 is plotted in Figure 2, which shows that λ increases with increasing Γ for a fixed $\tilde{\rho}_{\rm s}$, and also increases with increasing $\tilde{\rho}_{\rm s}$ for a certain value of Γ.

As mentioned in Section 2, the physical meaning of λ is the strength of energy advection on the equatorial plane. Obviously, for a certain fixed $\tilde{\rho}_{\rm s}$, Figure 2 shows that the advection on the equatorial plane increases with increasing Γ. In other words, the advection for $\Gamma>1$

is stronger than that for $\Gamma < 1$ at $\theta = \pi/2$. However, for the vertically integrated advection from the equatorial plane to the surface, it remains uncertain which one is stronger. The reason is that, with the relationship $q_{\rm adv}/q_{\rm vis} \propto |v_r|/v_\phi^2$ (see Equations 11-12 below), since Figure 1(a) shows that $|v_r|$ decreases and v_ϕ increases from $\theta = \pi/2$ to $\pi/6$, the advection strength will decrease from the equatorial plane to the surface. On the contrary, Figure 1(b) shows the opposite behavior of $|v_r|$ and v_ϕ, which means that the advection strength will increase from $\theta = \pi/2$ to $\pi/6$. Thus, the profile of the vertically integrated advection with Γ requires detailed numerical calculations. We will investigate this issue in next section.

4. Energy advection

In this section we will focus on the strength of energy advection. The viscous heating rate and the advective cooling rate per unit volume take the form (e.g., Gu et al. 2009):

$$q_{\rm vis} = \frac{9}{4}\frac{\alpha p_0 v_\phi^2 \tilde{\rho}^\Gamma}{r v_{\rm K}} \ , \tag{11}$$

$$q_{\rm adv} = -\frac{5-3\gamma}{2(\gamma-1)}\frac{p_0 v_r \tilde{\rho}^\Gamma}{r} \ , \tag{12}$$

where γ is the ratio of specific heats. For optically thin flows we adopt $\gamma = 1.5$, which corresponds to roughly equal amounts of gas and magnetic pressure (Narayan & Yi 1995b). Then, the vertical integration of the above two rates are the following:

$$Q_{\rm vis} = 2\int_{\frac{\pi}{6}}^{\frac{\pi}{2}} q_{\rm vis}\ r\sin\theta\ d\theta \ , \tag{13}$$

$$Q_{\rm adv} = 2\int_{\frac{\pi}{6}}^{\frac{\pi}{2}} q_{\rm adv}\ r\sin\theta\ d\theta \ . \tag{14}$$

The energy advection factor is defined as $f_{\rm adv} \equiv Q_{\rm adv}/Q_{\rm vis}$. The numerical methods to obtain the variation of $f_{\rm adv}$ with Γ are as follows. For a given value of $\tilde{\rho}_{\rm s}$ at $\pi/6$ (e.g., $\tilde{\rho}_{\rm s} = 0.01$), we solve Equation (7) and derive the vertical profile of $\tilde{\rho}$ and the parameter λ. Then, by Equations (4) and (6) we can obtain the profiles of v_r and v_ϕ. Thus, with Equations (11-14) we can derive the value of $f_{\rm adv}$. In the calculation the viscosity parameter is fixed as $\alpha = 0.1$.

The variation of $f_{\rm adv}$ with Γ for $\tilde{\rho}_{\rm s} = 0.1$, 0.01, and 0.001 is plotted in Figure 3. It is seen that the advection factor is far below unity, i.e., $f_{\rm adv} \lesssim 0.3$ for $0.1 < \Gamma < 1.7$. For the particular range $\tilde{\rho}_{\rm s} \lesssim 0.01$ and $0.5 < \Gamma < 1$, which was indicated by some simulation results (e.g., Figure 3 of Villiers et al. 2005), this figure shows even smaller advection factor with

$f_{\rm adv} < 0.1$. The above results illustrate that the advective cooling itself cannot balance the viscous heating.

For optically thin flows, the radiative efficiency η ($\equiv Q_{\rm rad}/Q_{\rm vis}$, where $Q_{\rm rad}$ is the radiative cooling rate per unit area) is roughly proportional to $\dot{M}$ (e.g., Kato et al. 2008, chap. 9.1, p. 290). Thus, for relatively low accretion rates (e.g., $\dot{M} \lesssim 10^{-3}\dot{M}_{\rm Edd}$), η will be quite small and the radiative cooling rate will be negligible compared with the viscous heating rate. Consequently, the viscous heating rate will be larger than the sum of the advective cooling rate and the radiative cooling one. In other words, no thermal equilibrium can be established under this situation. The contradiction may come from the original assumption that no outflow exists in the accretion system. We therefore propose that outflows ought to occur in optically thin flows with low accretion rates such as $\dot{M} \lesssim 10^{-3}\dot{M}_{\rm Edd}$. Moreover, the outflows should take away more than 70% of the thermal energy generated by viscous dissipation. As mentioned in Section 1, outflows have been found in accretion system by both observations and numerical simulations. Our analyses and numerical results may help to understand the mechanism, which is probably related to the insufficient energy advection.

5. Mass outflow rate

In this section we will estimate the total mass outflow rate based on the advection factor $f_{\rm adv}$. We define the quantity $\dot{M}_{\rm in}$ as the mass accretion rate of the inflow, which will increase with increasing r. For a small range $(r_0,\ r_0 + \Delta r)$, the mass outflow rate from this specific region can be expressed as

$$\Delta\dot{M}_{\rm out} = \dot{M}_{\rm in}|_{r=r_0+\Delta r} - \dot{M}_{\rm in}|_{r=r_0}\ . \tag{15}$$

Obviously, the total mass outflow rate can be written as

$$\dot{M}_{\rm out} = \dot{M}_{\rm in}|_{r=r_{\rm out}} - \dot{M}_{\rm in}|_{r=r_{\rm in}}\ , \tag{16}$$

where $r_{\rm in}$ and $r_{\rm out}$ are the inner and outer boundary, respectively. The above two equations show that, once the radial profile of $\dot{M}_{\rm in}$ is determined, the profile of mass outflow rate together with the total rate $\dot{M}_{\rm out}$ can be derived.

According to the spirit of this work, if the advective cooling could balance the viscous heating, i.e., $f_{\rm adv} = 1$, then the thermal equilibrium could be established and therefore it is not necessary for the occurrence of outflow. In other words, $\dot{M}_{\rm in}$ could be a constant if $f_{\rm adv} = 1$ were realized. We therefore assume that the inflow rate $\dot{M}_{\rm in}$ will satisfy the following equation:

$$\frac{d\ln\dot{M}_{\rm in}}{d\ln r} = \delta(1 - f_{\rm adv})\ , \tag{17}$$

where $\delta \lesssim 1$ is a dimensionless parameter. By the radial integration of the above equation we can obtain the ratio of inflow rate at the inner boundary to that at the outer boundary,

$$\frac{\dot{M}_{\rm in}|_{r=r_{\rm in}}}{\dot{M}_{\rm in}|_{r=r_{\rm out}}} = \left(\frac{r_{\rm in}}{r_{\rm out}}\right)^{\delta(1-f_{\rm adv})} . \tag{18}$$

The numerical results are shown in Figure 4, where $r_{\rm in} = 3r_{\rm g}$ and $r_{\rm out} = 10^3 r_{\rm g}$. The variation of such a ratio with Γ is plotted for $\delta = 1$, $1/2$, and $1/3$. It is seen that the ratio is not sensitive to Γ, but decreases rapidly with increasing δ, as can be inferred by Equation (18). The low values of this ratio implies that the outflow will be significant and even dominant, which agrees with the observation that only a small part of the original gas can be accreted by the supermassive black hole in the Milky Way. For a comparison with the numerical simulations of Yuan et al. (2012), as mentioned in Section 1, the inflow index s is in the range $[0.4,\ 0.7]$, which indicates that δ is probably in the range $[0.4,\ 1]$ (according to Equation 17) since our results show $f_{\rm adv} \lesssim 0.3$. In our understanding, the physical reason for δ less than unity may be related to the radiative cooling, which can balance a part of the viscous heating particularly for high accretion rates.

6. Conclusions and discussion

In the present paper, we have investigated the steady state, axisymmetric, optically thin accretion flows in spherical coordinates under the no-outflow assumption. We have found that the advective cooling rate is generally less than 30% of the viscous heating rate. As a consequence, for radiatively inefficient flows with low accretion rates such as $\dot{M} \lesssim 10^{-3}\dot{M}_{\rm Edd}$, no thermal equilibrium can be established since the viscous heating rate will be larger than the sum of the advective cooling rate and the radiative cooling one. We therefore argue that in such case outflows ought to occur and take away more than 70% of the thermal energy generated by viscous dissipation. Our results may help to understand the mechanism of outflows found in observations and numerical simulations.

On the other hand, for optically thick flows with extremely high accretion rates (e.g., $\dot{M} \gtrsim 10\dot{M}_{\rm Edd}$), the viscous heating is so strong that the radiative cooling will be quite small compared with the heating. The classic slim disk model predicts that the advective cooling will balance the viscous heating once the half-thickness of the disk H approaches the cylindrical radius R. However, Gu (2012) studied radiation pressure-supported disks with radiative transfer and showed that the disk will be extremely thick when advection is dominant. Moreover, for extremely high accretion rates, no thermal equilibrium solution was found, which also implies the occurrence of outflows. Here, it is easy to estimate the advection

strength for optical thick flows by Equation (12) and Figure 3. The main difference between optically thin and thick cases is related to γ, which is likely to be 4/3 for radiation pressure-dominated flows. In Section 4 we adopt $\gamma = 3/2$ for optically thin flows. Equation (12) implies that $q_{\rm adv}$ will be three times larger for $\gamma = 4/3$ than that for $\gamma = 3/2$. Thus, we can expect $f_{\rm adv} \lesssim 0.9$ for $0.1 < \Gamma < 1.7$. Moreover, with Figure 3 we can even expect $f_{\rm adv} < 0.2$ for the particular range $\tilde{\rho}_{\rm s} \lesssim 0.01$ and $0.5 < \Gamma < 1$, which is preferred according to simulation results. Consequently, under the no-outflow assumption, there will be no thermal equilibrium either for $\dot{M} \gtrsim 10\dot{M}_{\rm Edd}$. In other words, in such case outflows should also occur and take away the excess thermal energy, which is generated by viscous dissipation and cannot be balanced by advection plus radiation.

In our opinion, the strength of energy advection is a key point in accretion theory. Most previous works on this issue can be classified as the following two types. The first one is under cylindrical coordinates by using a Taylor expansion of gravitational force in the vertical direction, or equivalently by using a simple relation, i.e., $H = c_{\rm s}/\Omega_{\rm K}$, where $\Omega_{\rm K}$ is the Keplerian angular velocity (e.g., Abramowicz et al. 1988; Wang & Zhou 1999; Watarai et al. 2000; Sądowski et al. 2011). Such an approach may significantly magnify the original force and therefore greatly enlarge the strength of energy advection. The second one is under spherical coordinates by fixing a value of the local advection factor ($f'_{\rm adv} \equiv q_{\rm adv}/q_{\rm vis}$) in advance (e.g., Narayan & Yi 1995a; Xu & Chen 1997; Xue & Wang 2005; Jiao & Wu 2011). We would stress that both of the above two approaches may not properly derive the real strength of the advection. The method in the present work, however, provides a possible clue to investigate such a strength.

The present work is based on the constant α assumption. As shown by some simulations (e.g., Hirose et al. 2009; Jiang et al. 2014), however, the parameter α is not likely to be a constant in the vertical direction, which is probably relevant to the magnetic pressure. For instance, there may exist magnetically dominated coronae above the flow and therefore the constant α assumption may be violated. In addition, convection is not considered in this work, which may transfer energy in the vertical or radial direction. Thus, the above two issues may have quantitative influence on the present results.

As mentioned in the first section, outflows may be driven by several mechanisms such as radiation pressure and magnetic fields. In this work, we avoid the detailed mechanism to power outflows. Our no thermal equilibrium existence can be regarded as a necessary condition to illustrate that outflows are inevitable for both optically thin flows with low accretion rates and optically thick flows with extremely high accretion rates. In our opinion, it is worthy to check the strength of energy advection in simulations, particularly for those with strong outflows. Such a work may not be difficult since the values of physical quantities

in Equations (11-14) can be derived through simulations.

The author thanks Feng Yuan and De-Fu Bu for beneficial discussion, and the referee for helpful comments to improve the paper. This work was supported by the National Basic Research Program of China (973 Program) under grant 2014CB845800, the National Natural Science Foundation of China under grants 11222328 and 11333004, and the Fundamental Research Funds for the Central Universities under grant 20720140532.

REFERENCES

Abramowicz, M. A., Czerny, B., Lasota, J.-P., & Szuszkiewicz, E. 1988, ApJ, 332, 646

Blandford, R. D., & Payne, D. G. 1982, MNRAS, 199, 883

Gu, W.-M. 2012, ApJ, 753, 118

Gu, W.-M., & Lu, J.-F. 2007, ApJ, 660, 541

Gu, W.-M., Xue, L., Liu, T., & Lu, J.-F. 2009, PASJ, 61, 1313

Hirose, S., Krolik, J. H., & Blaes, O. 2009, ApJ, 691, 16

Jiang, Y.-F., Stone, J. M, & Davis, S. W. 2014, ApJ, 784, 169

Jiao, C.-L., & Wu, X.-B. 2011, ApJ, 733, 112

Kato, S., Fukue, J., & Mineshige, S. 2008, Black-Hole Accretion Disks: Towards a New Paradigm (Kyoto: Kyoto Univ. Press)

Narayan, R., Kato, S., & Honma, F. 1997, ApJ, 476, 49

Narayan, R., & Yi, I. 1994, ApJ, 428, L13

Narayan, R., & Yi, I. 1995a, ApJ, 444, 231

Narayan, R., & Yi, I. 1995b, ApJ, 452, 710

Ohsuga, K., & Mineshige, S. 2011, ApJ, 736, 2

Ohsuga, K., Mori, M., Nakamoto, T., & Mineshige, S. 2005, ApJ, 628, 368

Sądowski, A., Abramowicz, M., Bursa, M., Kluźniak, W., Lasota, J.-P., & Różańska A. 2011, A&A, 527, A17

Shakura, N. I., & Sunyaev, R. A. 1973, A&A, 24, 337

Villiers, J.-P., Hawley J. F., Krolik, J. H., & Hirose, S. 2005, ApJ, 620, 878

Wang, Q. D., Nowak, M. A., Markoff, S. B., et al. 2013, Science, 341, 981

Wang, J.-M., & Zhou, Y.-Y. 1999, ApJ, 516, 420

Watarai, K.-y., Fukue, J., Takeuchi, M., & Mineshige, S. 2000, PASJ, 52, 133

Xu, G., & Chen, X. 1997, ApJ, 489, L29

Xue, L., & Wang, J. 2005, ApJ, 623, 372

Yuan, F., & Bu, D.-F. 2010, MNRAS, 408, 1051

Yuan, F., Wu, M., & Bu, D. 2012, ApJ, 761, 129

This preprint was prepared with the AAS LaTeX macros v5.2.

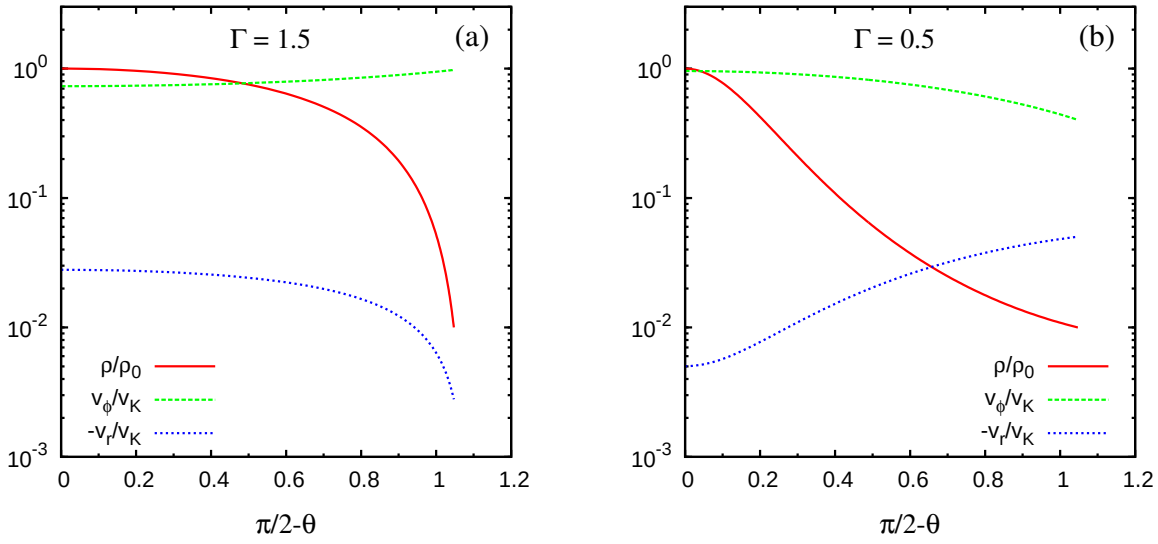

Fig. 1.— Variations of ρ, v_ϕ, and v_r for $\tilde{\rho}_{\rm s} = 0.01$: (a) $\Gamma = 1.5$; (b) $\Gamma = 0.5$.

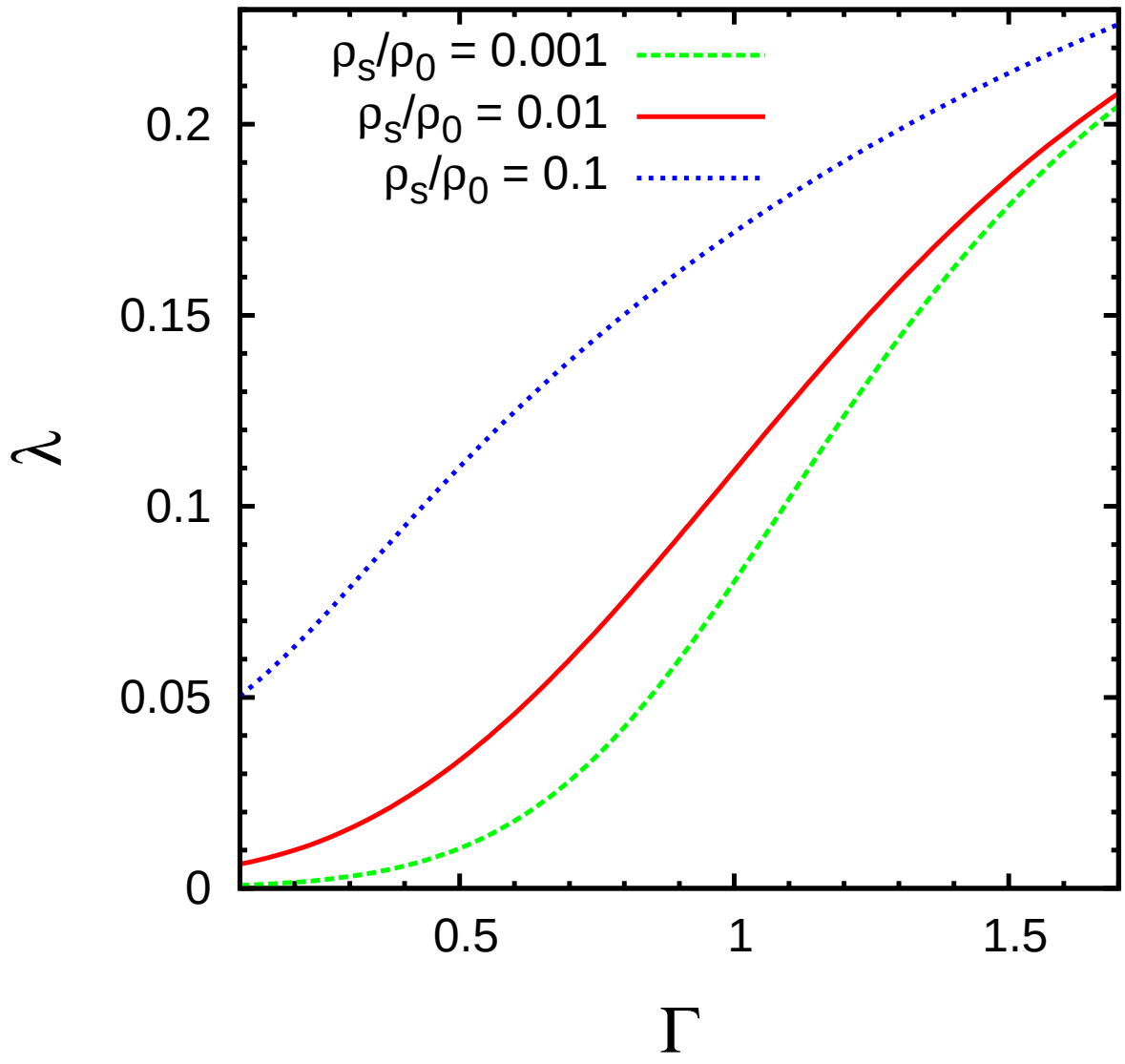

Fig. 2.— Variation of λ with Γ for $\tilde{\rho}_{\rm s} = 0.1$, 0.01, and 0.001.

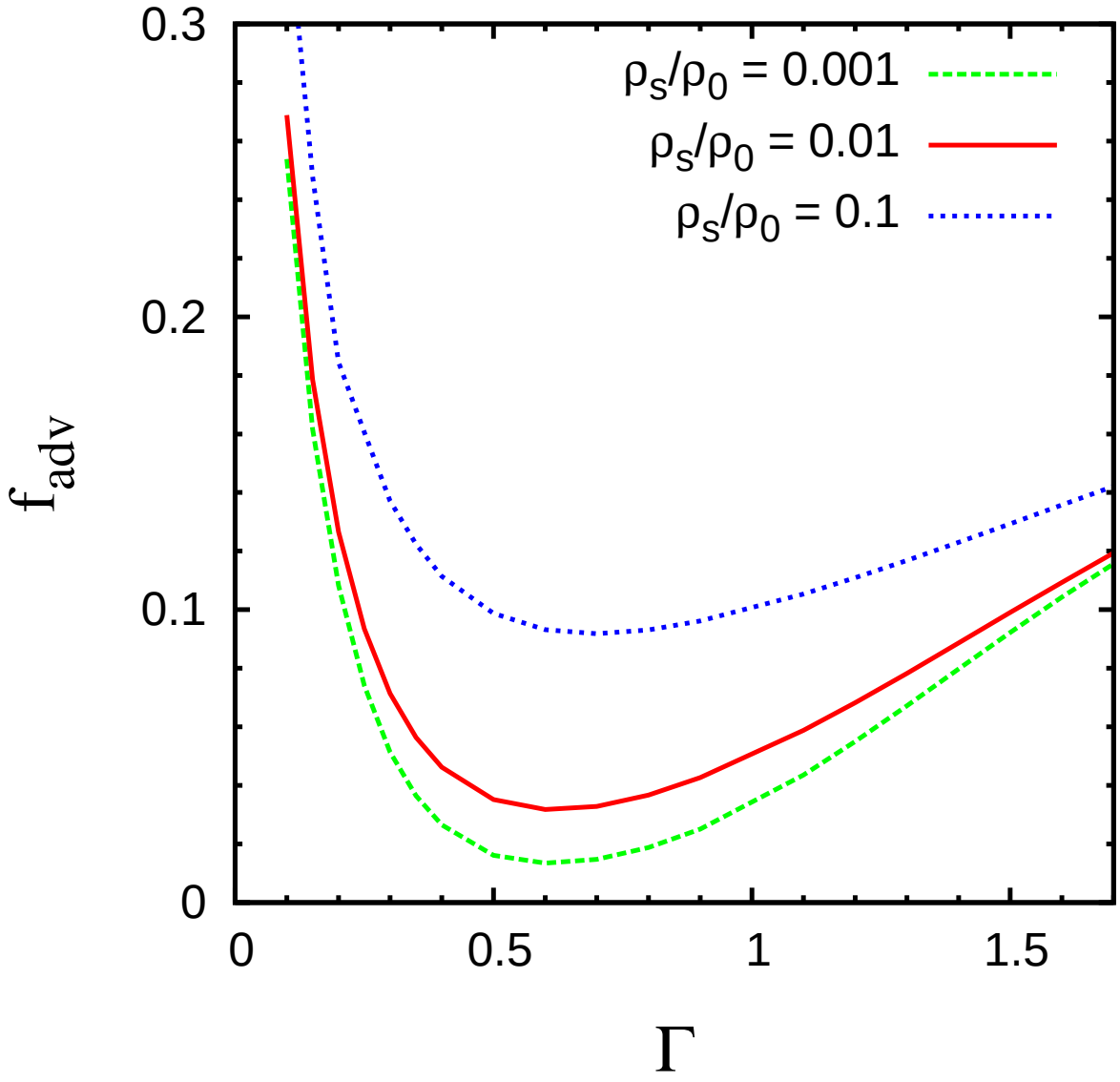

Fig. 3.— Variation of the advection factor $f_{\rm adv}$ with Γ for $\tilde{\rho}_{\rm s} = 0.1$, 0.01, and 0.001.

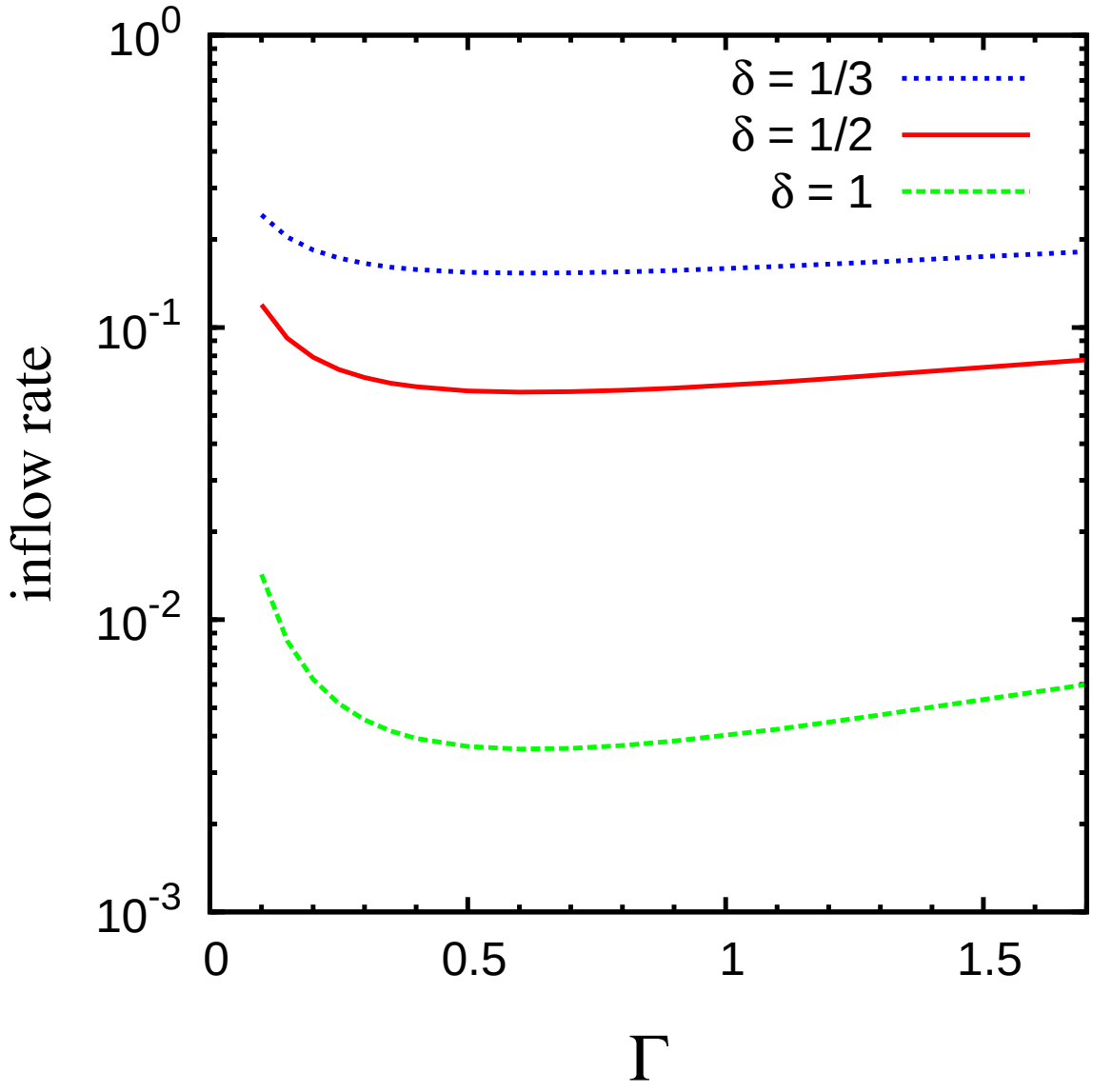

Fig. 4.— Variation of the ratio of inflow rate $(\dot{M}_{\rm in}|_{r=3r_{\rm g}})/(\dot{M}_{\rm in}|_{r=10^3r_{\rm g}})$ with Γ for $\delta = 1$, 1/2, and 1/3.